

Abrasive wear characteristics of plasma sprayed nanostructured alumina/titania coatings

You Wang^{*}, Stephen Jiang, Meidong Wang, Shihe Wang, T. Danny Xiao, Peter R. Strutt

Inframet Corporation, 20 Washington Avenue, North Haven, CT 06473, USA

Received 23 March 1999; received in revised form 19 August 1999; accepted 23 September 1999

Abstract

In this paper, the plasma spray technique was used to deposit coatings with reconstituted nanostructured $\text{Al}_2\text{O}_3/\text{TiO}_2$ powders. The abrasive wear resistance of the ceramic coatings was evaluated using diamond abrasives. The result showed that the abrasive wear resistance of the coatings produced using the nanostructured $\text{Al}_2\text{O}_3/\text{TiO}_2$ powders is greatly improved compared with the coating produced using the conventional $\text{Al}_2\text{O}_3/\text{TiO}_2$ powder (Metco 130). The highest abrasion resistance of the coating sprayed with nanostructured $\text{Al}_2\text{O}_3/\text{TiO}_2$ powder is about four times that of the coating sprayed with the conventional $\text{Al}_2\text{O}_3/\text{TiO}_2$ powder. Both as fabricated and after wear $\text{Al}_2\text{O}_3/\text{TiO}_2$ coatings were investigated by X-ray diffraction, SEM and indentation tests. The abrasive wear mechanism is also discussed. © 2000 Elsevier Science S.A. All rights reserved.

Keywords: Abrasive wear; Alumina; Titania

1. Introduction

Ceramic materials with high hardness and high resistance to thermal and corrosive conditions and relatively low densities offer many advantages over metallic and polymeric materials [1]. Oxide ceramics such as alumina, zirconia, titania, chromia, silica and yttria have been used widely as surface coating materials to improve wear, erosion, cavitation, fretting and corrosion resistance [2–4]. They are especially useful in applications where wear and corrosion resistances are required simultaneously. Thermal spray coating is one of the most common ways to improve the surface characteristics of materials. Plasma spraying is a widely used method among the thermal spray processes [5].

Because of their excellent properties, which are not available from metallic and cermet coatings, oxide coatings prepared using thermal spray processes have been widely used in U.S. Navy systems and by other industries.

For example, alumina which is a commonly used coating in the cutting tool industry, is the most effective coating in improving chemical or solution related wear [6,7]. Al_2O_3 -coated carbide tools exhibit a speed capability 2.5 times that of uncoated carbide tools [7].

In the past decade, most of the research in the field of nanomaterials has been focused on the synthesis and processing of powders and bulk materials. It is important to utilize the nanomaterials with new properties into industrial applications. In today's industry, there is a growing need of advanced coatings for machine parts working at various conditions. However, nanoparticle powders cannot successfully be thermal sprayed because of their low mass and their inability to be carried in a moving gas stream and deposited on a substrate. Realizing the potential high performance of nanostructured materials in engineered coating application, a process for the thermal spraying of nanostructured feeds, by which the nanoparticle powders can be reconstituted into spherical micron-sized granules that can be thermally sprayed has been developed [8,9]. The developed methodology involves the dispersion of the nanopowders into a colloidal suspension, followed by the addition of a binder and subsequent spray drying into granules. The methodology is very versatile in nature and

^{*} Corresponding author. E-mail: youwang@yahoo.com

has been used to make sprayable granules from metals, ceramics, and composite nanopowders. The details of the reconstitution of nanopowders have been given previously [8,9]. After reconstitution, the powder feedstocks should have a spherical or near-spherical morphology, be dense sintered particles, with a narrow particle size distribution, e.g., 15 to 100 μm in diameter, to ensure good flowability in the existing powder feeding systems.

2. Experimental

2.1. Thermal spray

Thermal spray processes of the reconstituted sprayable feedstocks and conventional ones are carried out with a Metco 9MB plasma gun. The details of powder compositions and the test data of coatings are shown in Table 1. Ceramic coatings were deposited from 250 to 600 μm thick on mild carbon steel coupons. The coupons were blasted to remove rust and the surfaces are cleaned prior to thermal spray deposition. The depositions were performed using a GM-Fanuc six-axis thermal spray robot, a two-axis specimen stage, and a computer control system.

The parameters for thermal spraying of nanostructured ceramic coatings were adjusted to (i) minimize the coarsening of the nanograins, (ii) control chemical reactions of materials, and (iii) control phase stability at high temperature. The parameters included the ratio of gas flow rate, powder feed rate, spray distance, number of passes, and powder pre-sintering characteristics. Here, for nanostructured $\text{Al}_2\text{O}_3/\text{TiO}_2$, $\text{Al}_2\text{O}_3/\text{TiO}_2 + \text{CeO}_2$, $\text{Al}_2\text{O}_3/\text{TiO}_2 + \text{CeO}_2 + \text{ZrO}_2$ powders, the plasma deposition parameters are as follows: (a) primary Ar gas pressure is about 690 kPa, (b) secondary H_2 gas pressure is about 380 kPa, (c) Ar gas flow rate (SCFH) is 120, (d) powder carrier gas flow rate (SCFH) is 40–70, (e) powder feed rate is 400–900 g/h, (f) current is 600 A, (g) voltage is 65 V, (h) gun moving speed is 500 mm/s, (i) spray distance is about 100 mm, and (j) thermal spraying 10 passes after one cycle preheating. For the depositing of conventional $\text{Al}_2\text{O}_3/\text{TiO}_2$

powder, the plasma spray parameters used are based on Metco's specification for Metco 130 powder [10].

2.2. Abrasive wear test

The abrasive wear tests were performed on a modified grinding/polishing machine (Struers grinding/polishing system comprised a RotoPol-22 controlled grinding and polishing discs equipped with a RotoForce-4 specimen mover and a Multidoser with a RotoCom memory unit. After modification, the system is similar to a computer controlled pin-on-disk wear tester) at room temperature. Prior to the wear tests, coating surfaces were polished using successively smaller diamond abrasives (i.e., 9, 3 and 1 μm). The tests were conducted under a normal load of 90 N and at a sliding speed of 2.67 m/s. Coated samples were used as pins (cylindrical samples) with a flat surface of 32 mm in diameter. Before wear testing, all samples were cleaned with acetone. A 40- μm diamond abrasive pad with diameter of 170 mm was used as disk. It was dressed and cleaned before each experiment, and lubricated with water during the tests.

Abrasion rates (wear rates) are calculated using the mean measurement value of three samples in terms of the volume of material removed (in mm^3) per unit load (N), and distance of sliding against the diamond abrasive pad (mm), in unit of $\text{mm}^3/\text{N mm}$.

2.3. Characterization of the sprayed coatings

Crystal structures were analyzed using a Siemens D5005 computer-interfaced X-ray diffraction system at glancing angle geometry. Surface morphologies of worn surfaces and cross-sections of these coatings were examined using scanning electron microscope (JEOL JSM-840A). Microhardness of these coatings was determined under a load of 300 g using a Leco M-400-G2 hardness tester. Indentation crack lengths on the cross-sections of the coatings were also measured on this hardness tester.

Table 1
Powder composition and characteristics of testing coatings

Coating	Powder composition	Powder type	Powder feed rate (g/h)	Coating hardness (HV_{300})	Coating thickness (μm)
C1	$\text{Al}_2\text{O}_3/13\% \text{TiO}_2$	Commercial powder (Metco 130)		1057	500–600
N1	$\text{Al}_2\text{O}_3/13\% \text{TiO}_2$	nanostructured powder	410–770	1034	350–450 ^a
N2	$\text{Al}_2\text{O}_3/13\% \text{TiO}_2 + \text{CeO}_2$	nanostructured powder	410–635	995	300–450 ^a
N3	$\text{Al}_2\text{O}_3/13\% \text{TiO}_2 + \text{CeO}_2 + \text{ZrO}_2$	nanostructured powder	365–455	1044	250–350 ^a

^aThe thickness of the coatings can be built up to 500–600 μm by increasing spraying passes.

3. Experimental results and discussion

3.1. SEM observation of coating cross-sections

Fig. 1 shows the cross-section SEM micrographs of coatings produced with under various conditions. These conditions are:

- (i) nanostructured $n\text{-Al}_2\text{O}_3/\text{TiO}_2$ powder;
- (ii) nanostructured $n\text{-Al}_2\text{O}_3/\text{TiO}_2 + \text{CeO}_2$ powder;
- (iii) nanostructured $n\text{-Al}_2\text{O}_3/\text{TiO}_2 + \text{CeO}_2 + \text{ZrO}_2$ powder;
- and (iv) conventional $\text{Al}_2\text{O}_3/\text{TiO}_2$ (Metco 130) powder.

It can be seen from Table 1 that the microhardness of the coatings sprayed with nanostructured $\text{Al}_2\text{O}_3/\text{TiO}_2$ powder is similar to that of the coating sprayed with conventional $\text{Al}_2\text{O}_3/\text{TiO}_2$ powder. And, it can be seen that the morphologies and density of these coatings via SEM examination seem are also similar, as shown in Fig. 1. Despite the coating hardness and microstructural similarities at this level of magnification, the wear resistances are quite dif-

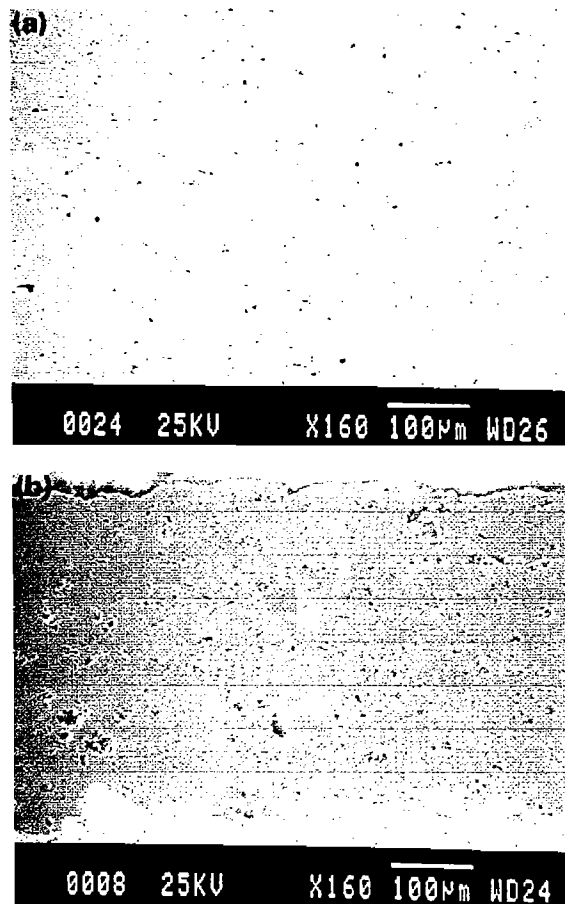


Fig. 1. Scanning electron micrographs of the cross-sections of coatings sprayed with: (a) conventional $\text{Al}_2\text{O}_3/\text{TiO}_2$ (Metco 130) powder; (b) $n\text{-Al}_2\text{O}_3/\text{TiO}_2$ powder; (c) $n\text{-Al}_2\text{O}_3/\text{TiO}_2 + \text{CeO}_2$ powder; (d) $n\text{-Al}_2\text{O}_3/\text{TiO}_2 + \text{CeO}_2 + \text{ZrO}_2$ powder.

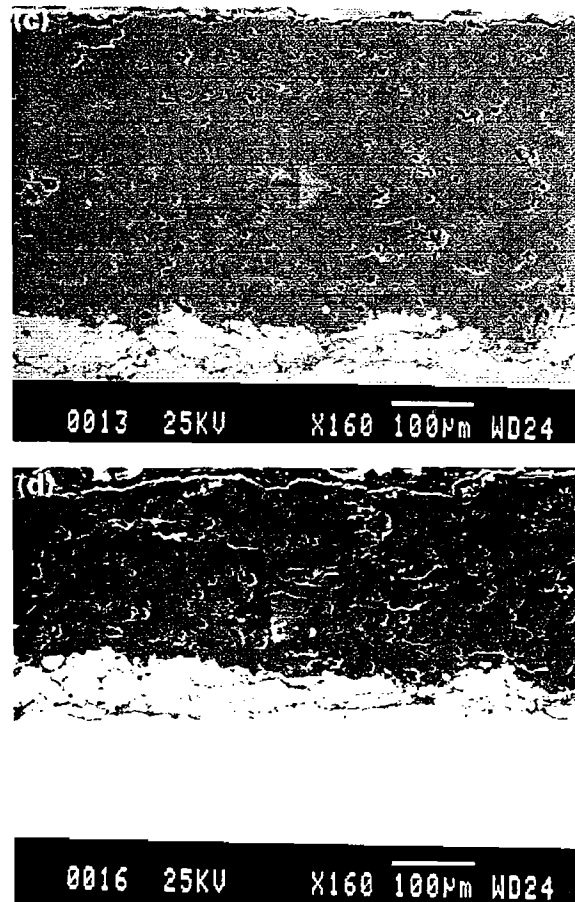


Fig. 1 (continued).

ferent. Abrasive wear tests via diamond abrasives indicated that the coatings sprayed with nanostructured $\text{Al}_2\text{O}_3/\text{TiO}_2$ powder are more resistant to wear than the coating sprayed with conventional $\text{Al}_2\text{O}_3/\text{TiO}_2$ powder, the details are given below.

Observation with higher magnification SEM can provide further information about the microstructures of the coatings sprayed with nanostructured $\text{Al}_2\text{O}_3/\text{TiO}_2$ powders. It can be found from Fig. 2 that there were nano-scale and submicron-scale microstructures in the coatings, forming a skeleton-like structure. The nano-scale and submicron-scale skeleton structures must have played a very important role during wear. This will be discussed later.

3.2. X-ray diffraction results before and after wear tests

Fig. 3 shows the X-ray diffraction patterns of the as-sprayed ceramic coatings. It is obvious that $\gamma\text{-Al}_2\text{O}_3$ is the predominant phase in all the as-sprayed coatings. However, there were differences in the microstructures of the five different coatings. It can be seen from Fig. 3 that the strongest peak is $\gamma\text{-Al}_2\text{O}_3$ (400) in the conventional $\text{Al}_2\text{O}_3/\text{TiO}_2$ coating (C1), whereas the coating sprayed

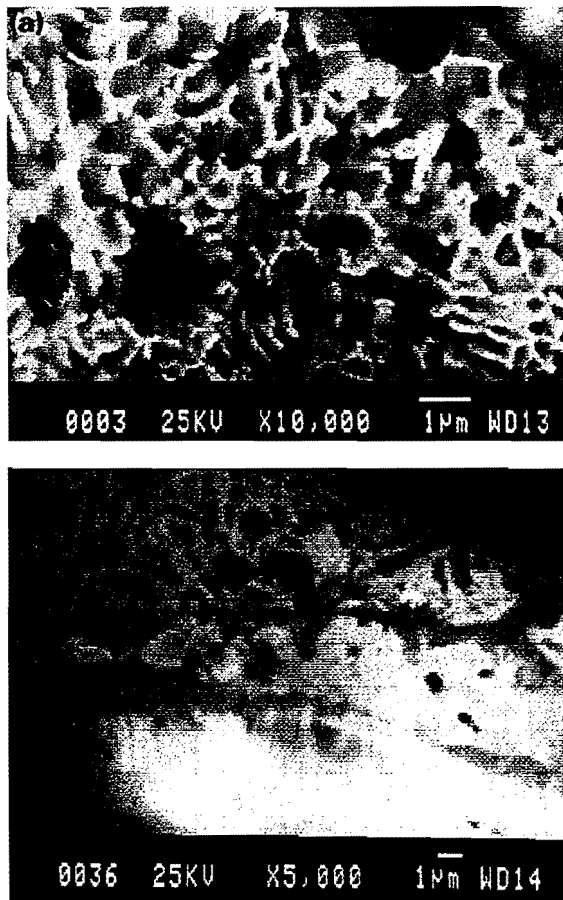


Fig. 2. Higher magnification scanning electron micrographs of the cross-section microstructures of coatings sprayed with nanostructured $\text{Al}_2\text{O}_3/\text{TiO}_2$ powders. (a) $n\text{-Al}_2\text{O}_3/\text{TiO}_2$ powder; (b) $n\text{-Al}_2\text{O}_3/\text{TiO}_2 + \text{CeO}_2$ powder.

with nanostructured $\text{Al}_2\text{O}_3/\text{TiO}_2 + \text{CeO}_2 + \text{ZrO}_2$ powder (N3) also forms $\gamma\text{-Al}_2\text{O}_3$ but with preferential growth in the 440 direction. This indicates that there are preferential growth directions in all coatings sprayed. But the preferential growth direction of the coating sprayed with conventional $\text{Al}_2\text{O}_3/\text{TiO}_2$ powder is obviously different from that of the coatings sprayed with nanostructured $\text{Al}_2\text{O}_3/\text{TiO}_2$ powder. And, the relative intensities of $\gamma\text{-Al}_2\text{O}_3$ (440) peaks in the coatings sprayed with nanostructured $\text{Al}_2\text{O}_3/\text{TiO}_2$ powder increased due to the addition of CeO_2 or $\text{CeO}_2 + \text{ZrO}_2$ into the $\text{Al}_2\text{O}_3/\text{TiO}_2$ powder. This result indicates that the addition of CeO_2 or $\text{CeO}_2 + \text{ZrO}_2$ into the $\text{Al}_2\text{O}_3/\text{TiO}_2$ powder changed the surface textures. The formation of surface texture i.e., certain crystal orientation should have an important influence on wear properties of $\text{Al}_2\text{O}_3/\text{TiO}_2$ coatings.

Fig. 4 is the XRD results of worn surfaces of different coatings after wear testing. Comparing the XRD patterns before and after wear testing (Figs. 3 and 4), it is found that the diffraction intensities of $\gamma\text{-Al}_2\text{O}_3$ (440) change. The results of the experiments show that friction and wear

process of $\text{Al}_2\text{O}_3/\text{TiO}_2$ coatings must be accompanied by a texture change on the worn surface. In addition, the increase of $\alpha\text{-Al}_2\text{O}_3$ diffraction intensities, e.g., (024), (104), (113) and (116), can be found after wear testing.

3.3. Coating wear resistances

Wear volumes of different $\text{Al}_2\text{O}_3/\text{TiO}_2$ coatings are presented in Fig. 5. It can be found that the wear rates of the coatings are remarkably different. The calculated wear rate of the coating sprayed with conventional $\text{Al}_2\text{O}_3/\text{TiO}_2$ powder is $1.461 \times 10^{-7} \text{ mm}^3/\text{N mm}$. While the calculated wear rates of the coatings sprayed with nanostructured $\text{Al}_2\text{O}_3/\text{TiO}_2$ powders are $6.112 \times 10^{-8} \text{ mm}^3/\text{N mm}$ for coating N1, $4.727 \times 10^{-8} \text{ mm}^3/\text{N mm}$ for coating N2 and $3.079 \times 10^{-8} \text{ mm}^3/\text{N mm}$ for coating N3, respectively. It can be concluded that C1, the conventional coating, has the lowest wear resistance. However, the wear resistance of N1, a coating sprayed with nanostructured $\text{Al}_2\text{O}_3/\text{TiO}_2$ powder, is about two times that of C1. It should be noticed that the wear resistance of thermal sprayed $\text{Al}_2\text{O}_3/\text{TiO}_2$ coatings can be remarkably in-

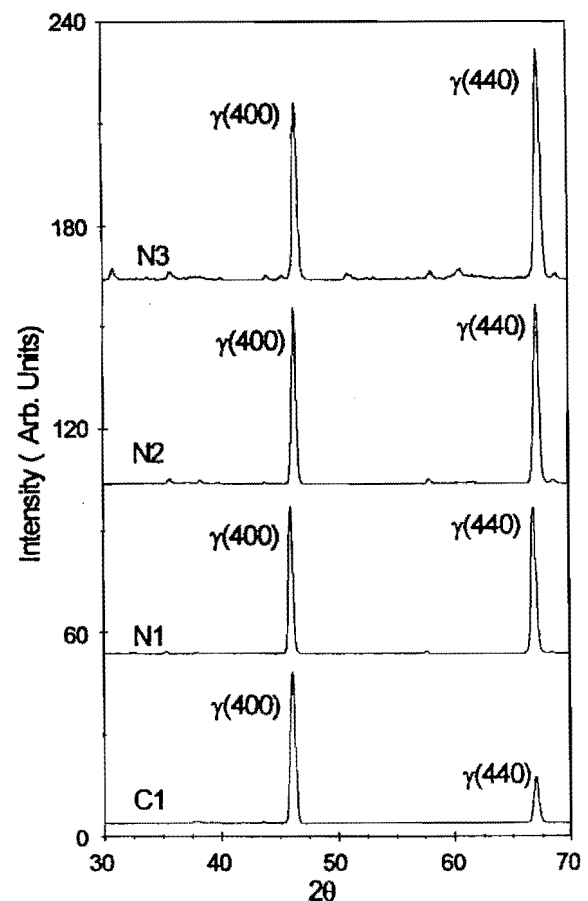


Fig. 3. X-ray diffraction patterns of the ceramic coatings before wear tests.

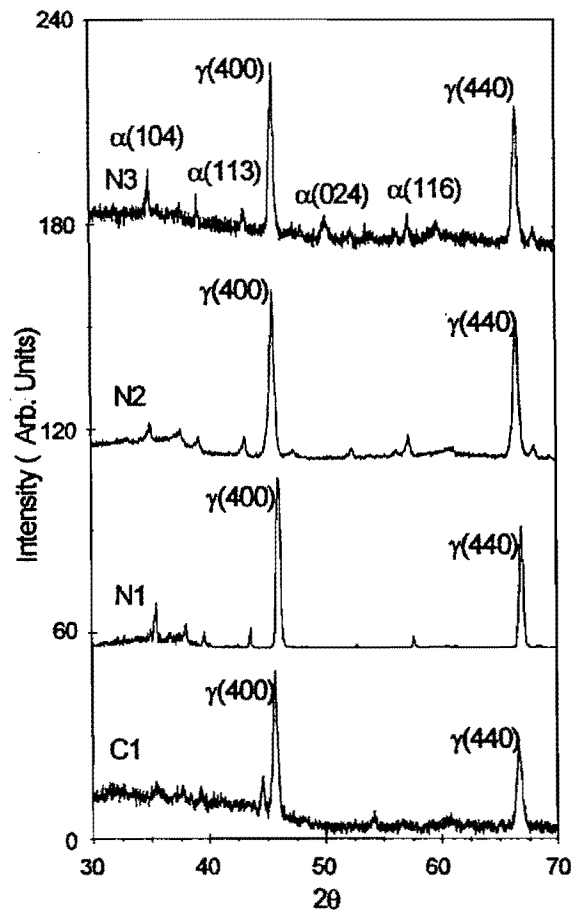


Fig. 4. XRD results obtained from worn surfaces of different coatings after wear tests.

created by the addition of CeO_2 or $\text{CeO}_2 + \text{ZrO}_2$ into the $\text{Al}_2\text{O}_3/\text{TiO}_2$ powder. For example, the wear resistance of the coating can be increased two times or more by adding CeO_2 to the $\text{Al}_2\text{O}_3/\text{TiO}_2$ powder. Moreover, the wear resistance of the coating can be increased more than three times with the addition of $\text{CeO}_2 + \text{ZrO}_2$ into the $\text{Al}_2\text{O}_3/\text{TiO}_2$ powder.

These data clearly indicate that nanostructured coatings have great potential to provide substantial improvement in wear resistance over conventional counterparts.

3.4. Worn surface morphology

Fig. 6 shows the worn surface morphologies of the $\text{Al}_2\text{O}_3/\text{TiO}_2$ coatings. There is an obvious difference between the coating sprayed with conventional $\text{Al}_2\text{O}_3/\text{TiO}_2$ powder and those with nanostructured $\text{Al}_2\text{O}_3/\text{TiO}_2$ powders. The friction track on the conventional material coating is rough. Some grooves, plastic deformation and intergranular microfracture features can be found on the worn surface of the coating sprayed with conventional $\text{Al}_2\text{O}_3/\text{TiO}_2$ powder, as shown in Fig. 6a. However, the coatings sprayed with nanostructured

$\text{Al}_2\text{O}_3/\text{TiO}_2$ powders are smooth without obvious grooves, deformation and microfracture features, as shown in Fig. 6b,c,d.

Cracks may propagate either along grain boundaries or through grains as intracrystalline cleavage. Since the energy of grain boundary fracture is about one half of that for crystalline cleavage [11], the former process is favored. SEM micrographs of higher magnification provide information on the nature of damage and the mechanism of material removal. It can be seen from Fig. 6a and Fig. 7a that the dominating mechanism of material removal for the coating sprayed with conventional $\text{Al}_2\text{O}_3/\text{TiO}_2$ powder should be a combination of (i) grain dislodgment due to grain boundary fracture and (ii) lateral crack chipping. However, the dominating mechanism of material removal for the coatings sprayed with nanostructured $\text{Al}_2\text{O}_3/\text{TiO}_2$ powders is grain dislodgment as suggested by Xu and Jahanmir [12], as shown in Fig. 6b,c,d and Fig. 7b,c,d. Here, the situation of wear testing is different from that cited by Xu and Jahanmir. This is a more rapid process of damage accumulation rather than the scratching with a diamond indenter. This is a rapid wear stage characterized by microfracture and grain pull-out [13]. So in this case, the calculated wear rates of the coatings show that the wear processes are severe wear due to the wear rates are greater than $2 \times 10^{-8} \text{ mm}^3/\text{N mm}$ [14].

It can also be noticed from the worn surfaces shown in Fig. 7 that the grain size of the coating sprayed with conventional $\text{Al}_2\text{O}_3/\text{TiO}_2$ powder is about several microns, while the grain size of the coatings sprayed with nanostructured $\text{Al}_2\text{O}_3/\text{TiO}_2$ powders is usually less than $1 \mu\text{m}$ (from $0.1\text{--}1.0 \mu\text{m}$), and a significant fraction of the grains are less than 50 nm .

3.5. Effect of microhardness and toughness on wear resistance

A variety of wear mechanisms exists, based on a large amount of the research work conducted on coating and

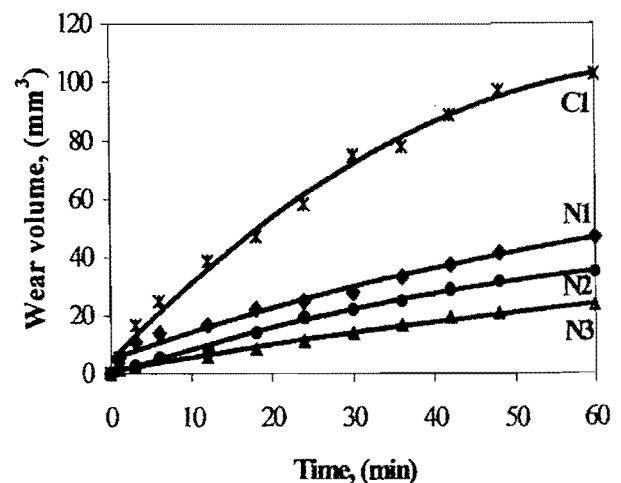


Fig. 5. Wear volumes of different $\text{Al}_2\text{O}_3/\text{TiO}_2$ coatings.

bulk materials. It is commonly indicated that the wear resistance of a material is closely related to its microhardness, toughness, microstructure, defect content and the ratio of its hardness to the hardness of the abrasive [15–19]. Many studies have suggested that a high hardness is desirable for both brittle and ductile materials, while a brittle material benefits further from a high toughness [13,16].

Fig. 8 shows the relationship between the wear volume and the hardness of the coatings. It should be noted from the results shown in Figs. 5 and 8 that there is no simple relationship between the wear resistance and the hardness of the coatings. This means that the abrasive wear mechanism of the coatings not only depends on coating hardness and density, but also on particle size, type of the powder used, coating microstructure, as well as microstructural change during wear testing. Thus, the wear resistance of the $\text{Al}_2\text{O}_3/\text{TiO}_2$ coating can be changed significantly by selecting different powder process methods or by adding different additives, even if the hardness is almost the same.

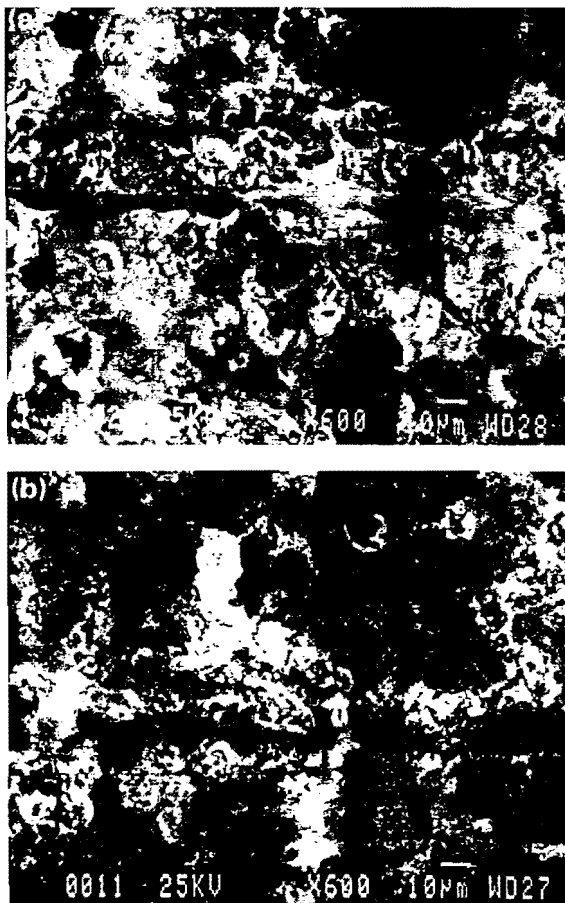


Fig. 6. Worn surface morphologies of $\text{Al}_2\text{O}_3/\text{TiO}_2$ coatings sprayed with: (a) conventional $\text{Al}_2\text{O}_3/\text{TiO}_2$ (Metco 130) powder; (b) $n\text{-Al}_2\text{O}_3/\text{TiO}_2$ powder; (c) $n\text{-Al}_2\text{O}_3/\text{TiO}_2 + \text{CeO}_2$ powder; (d) $n\text{-Al}_2\text{O}_3/\text{TiO}_2 + \text{CeO}_2 + \text{ZrO}_2$ powder.

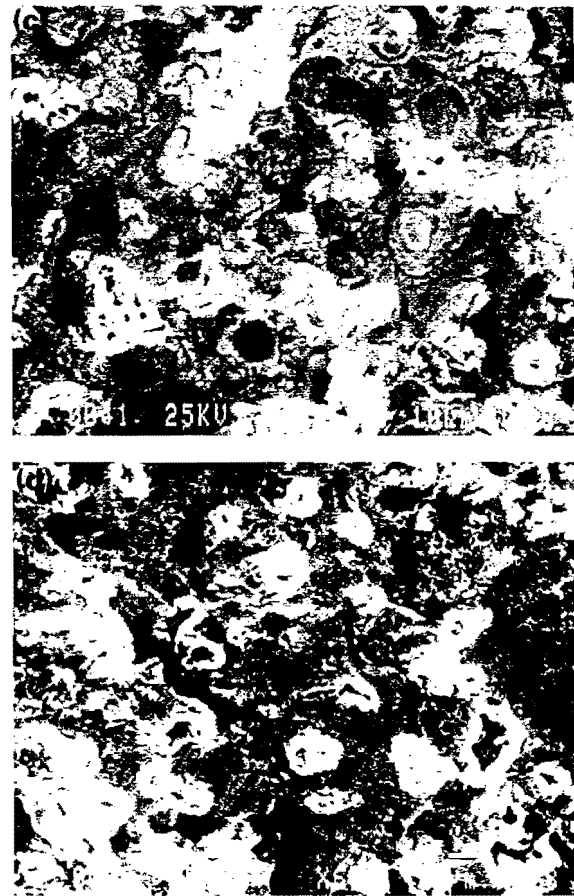


Fig. 6 (continued).

A possible reason for the conventional $\text{Al}_2\text{O}_3/\text{TiO}_2$ coating exhibits the lowest wear resistance is their brittleness. SEM examination of the coating cross-sections shows that some cracks have already been produced in the conventional $\text{Al}_2\text{O}_3/\text{TiO}_2$ coating before indentation and wear testing, as shown in Fig. 9. The measurements of indentation cracking length which relating to toughness on the various coatings were done in this experiment. The relationship between the wear volume and the indentation cracking length on the cross-sections of the coatings is shown in Fig. 10. Therefore, it can be concluded that the abrasive wear resistance of the $\text{Al}_2\text{O}_3/\text{TiO}_2$ ceramic coatings is strongly dependent on the toughness of the coatings.

3.6. Effects of microstructure and grain size on wear resistance

Wear is such a complex process that many factors will influence it. In a certain case, one or more factors will dominate the wear resistance of the materials, but they change as conditions change. In addition to the effect of toughness and hardness, the microstructure of ceramics,

especially grain size, has an immense influence on the wear resistance [13,16,19]. In our case, it was noticed that the microstructures in coatings changed during the wear process. The results of XRD tests showed that the phase changed more or less from $\gamma\text{-Al}_2\text{O}_3$ to $\alpha\text{-Al}_2\text{O}_3$. The $\gamma\text{-Al}_2\text{O}_3$ is an unstable phase, absorbing the friction heat and partially becoming the stable phase $\alpha\text{-Al}_2\text{O}_3$. It can be found that not only the intensities of $\gamma\text{-Al}_2\text{O}_3$ (440) decreased but also the intensities of $\alpha\text{-Al}_2\text{O}_3$, e.g., (024), (104), (113) and (116), increased after wear testing. The changes in microstructures are more significant in the nanostructured coatings than in the conventional (C1) coating. It is believed that this phase transformation also has an important effect on the wear process. As mentioned above, there was a preferential growth in the coatings due to the process of powders and additives, i.e., the original microstructure of individual coatings was different. This preferential growth certainly affected the wear behavior of individual coating to some degree. It is safe to say that

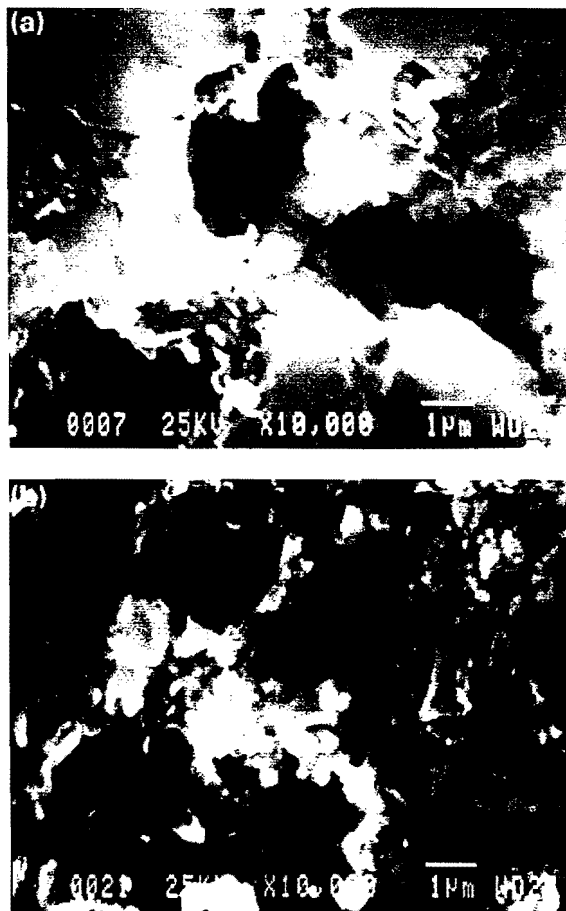


Fig. 7. Higher magnification scanning electron micrographs of the worn surface morphologies of coatings sprayed with: (a) conventional $\text{Al}_2\text{O}_3/\text{TiO}_2$ (Metco 130) powder; (b) $n\text{-Al}_2\text{O}_3/\text{TiO}_2$ powder; (c) $n\text{-Al}_2\text{O}_3/\text{TiO}_2 + \text{CeO}_2$ powder; (d) $n\text{-Al}_2\text{O}_3/\text{TiO}_2 + \text{CeO}_2 + \text{ZrO}_2$ powder.

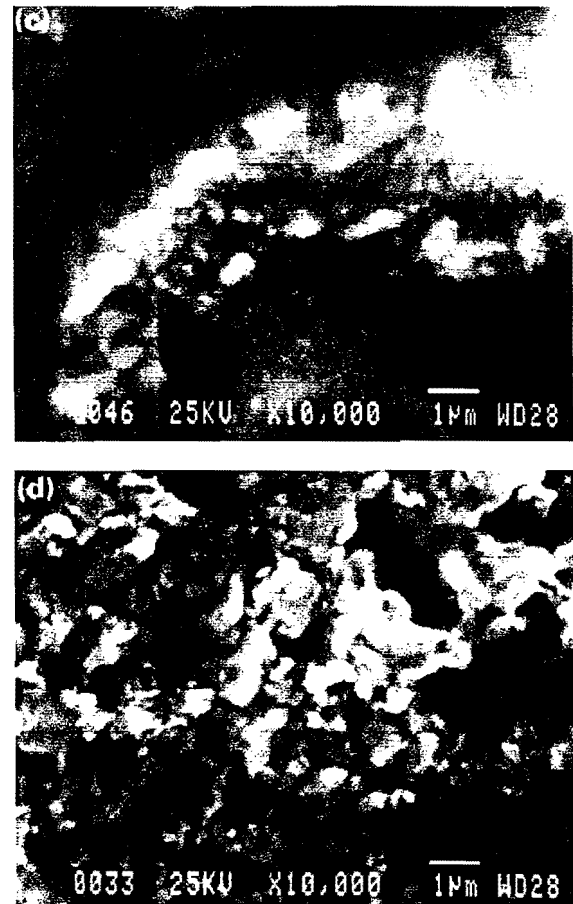


Fig. 7 (continued).

different microstructures of coatings make different contribution to the wear resistance.

It is generally recognized that the wear of polycrystalline alumina materials varies significantly with mean grain size G , wear rate W increasing rapidly with increasing grain size [20]. Numerous studies have indicated that fine-grained ceramics have lower wear rates than coarse-grained ceramics in both sliding [13,16] and erosive wear [21,22]. For example, reducing the grain size of Al_2O_3 from 20 to 4 μm has led to a five-fold increase in the transition time from a slow wear stage characterized by plastic deformation and grooving to a rapid wear stage characterized by microfracture and grain pull-out [13]. The wear rate in the slow wear stage is literally negligible. Thus, the longer the slow wear stage, the longer the life of the wear parts. At the slow wear stage, the damage due to the plastic deformation within individual grains accumulates, which in turn augments the pre-existing thermal stress at grain boundaries due to mismatches in thermal expansion coefficients and triggers the onset of the grain boundary cracking and grain pull-out [13,16]. The stress at grain boundaries can be dramatically relaxed in nano-scale regimes due to the enhanced grain boundary diffusion.

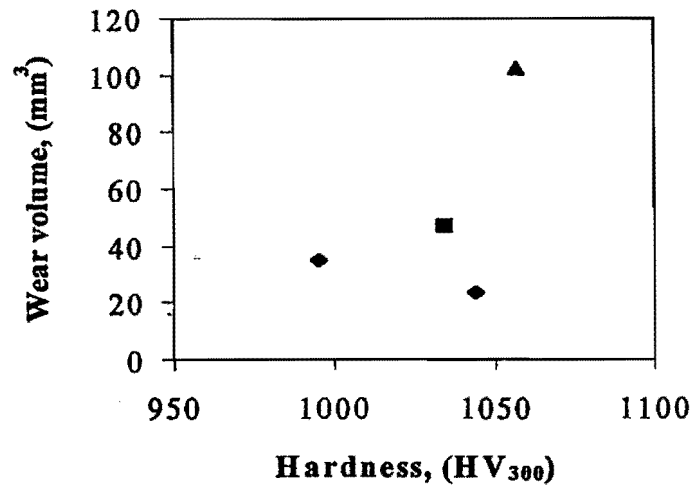


Fig. 8. The relationship between the wear volume and the hardness of the coatings.

Therefore, it is expected that the stress build-up at the grain boundaries due to the plastic deformation within individual grains will be slowed down substantially by reducing the grain size to nano-scale regimes. Thus, the

onset of the grain boundary cracking and grain pull-out will be postponed and a ceramic material with a long slow wear stage and superior wear resistance will result. Microfracture (e.g., grain boundary cracking and grain pull-out) is by far the most important source of wear in ceramic materials [23]. This is because, unlike metallic materials, most ceramics are inherently brittle. Nevertheless, microscale plastic deformation has been observed in many ceramics such as Al_2O_3 [16], ZrO_2 [24], SiO_2 [21] and Si_3N_4 [21] during sliding and erosive wear. A major cause of microfracture in ceramics is the dislocation pile-up against grain boundaries that in turn acts as stress concentration and triggers grain boundary cracking and grain pull-out [23]. The smaller the grain size, the finer the flaws and the higher the external stress required to induce grain boundary cracking and grain pull-out. As indicated, the smaller the grain, the more resistant it is to fracture [25,26]. Thus, with fine flaws, the enhanced grain boundary diffusion and the associated stress relaxation, nanostructured ceramics or ceramic coatings are expected to have better wear and erosion resistance than conventional counterparts. The results of abrasive wear tests have confirmed this.

From the XRD results shown in Figs. 3 and 4, the coatings with different original structures trend toward the same structure during wear. It can be inferred from this that the difference in wear resistance of different coatings is related to the processes of structural changes. That is to say, different coatings show different structural change processes and different energy consumption. If a coating consumes more energy during the process, the coating will show better wear resistance. In the present experiments, the formation of the microstructures (including phase, grain size and surface texture etc.) and their changes during wear has not yet been examined systematically. In addition, the energy consumption has not been measured. Further detail works are needed. However, the influences

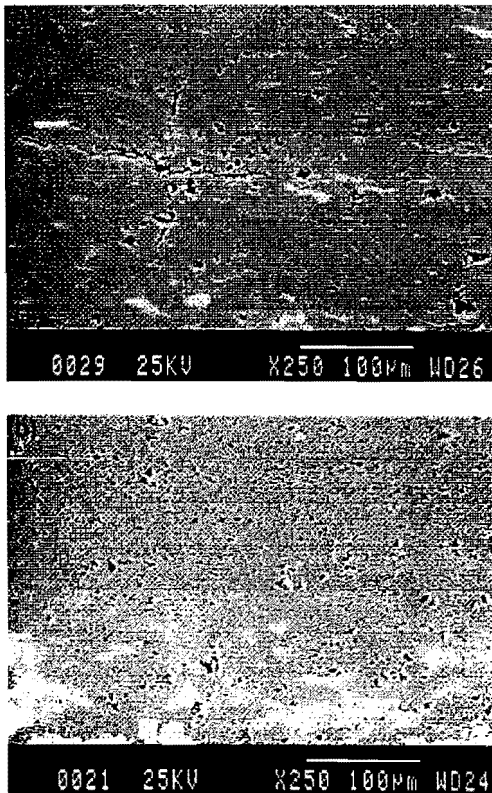


Fig. 9. Scanning electron micrographs of the cross-section of $\text{Al}_2\text{O}_3/\text{TiO}_2$ coatings: (a) conventional coating shows that some cracks have already been produced before indentation and wear testing; (b) nanostructured coating.

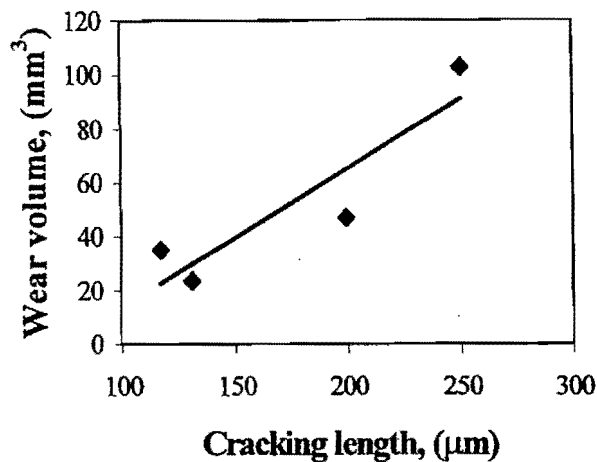


Fig. 10. The relationship between the wear volume and the indentation cracking length on the cross-sections of the coatings.

of the processes on wear resistance are described. The wear resistance of different coatings is dependent on the processes that consume energy during wear.

For different coatings, the energy consumption during wear under the same conditions is different due to their microstructural characteristics. It is suggested that the energy consumption of coatings sprayed with nanostructured $\text{Al}_2\text{O}_3/\text{TiO}_2$ powders may be greater than those of coating sprayed with conventional $\text{Al}_2\text{O}_3/\text{TiO}_2$ powder, due to their large microfracture resistance of the very small grain size and the big microstructural change during wear. Perhaps grain boundaries are one of destination where absorbed energy is stored in forms of thermal movement of atoms and defects there. The larger the boundary volume, the more energy could be absorbed, therefore the finer grain size, the greater wear resistance the materials might offer. Nevertheless, it is a right way to improve the wear resistance by fine grain route.

4. Conclusions

(1) Nano-scale and submicron-scale skeleton microstructures can be formed in the coatings sprayed with nanostructured $\text{Al}_2\text{O}_3/\text{TiO}_2$ powders, and play a very important role in wear process.

(2) X-ray diffraction showed that the sprayed $\text{Al}_2\text{O}_3/\text{TiO}_2$ coatings consisted mainly of $\gamma\text{-Al}_2\text{O}_3$ phase. The X-ray diffraction result also showed that the preferential crystal growth of the coating sprayed with conventional $\text{Al}_2\text{O}_3/\text{TiO}_2$ powder is obviously different from that of the coatings sprayed with nanostructured $\text{Al}_2\text{O}_3/\text{TiO}_2$. The addition of CeO_2 or $\text{CeO}_2 + \text{ZrO}_2$ into the $\text{Al}_2\text{O}_3/\text{TiO}_2$ powder can promote the formation of surface texture. The surface texture has an important influence on the wear properties of $\text{Al}_2\text{O}_3/\text{TiO}_2$ coatings. The results also showed that friction and wear process of

$\text{Al}_2\text{O}_3/\text{TiO}_2$ coatings is accompanied by a texture change on the wearing surface. The coatings with different original structures trend towards the same stable structure, $\alpha\text{-Al}_2\text{O}_3$, during abrasive wearing.

(3) Abrasive wear data indicate that the coatings sprayed with nanostructured $\text{Al}_2\text{O}_3/\text{TiO}_2$ powders have the potential to provide substantial improvements in wear resistance over conventional counterparts. The wear resistance of the coating can be three times increased with the addition of $\text{CeO}_2 + \text{ZrO}_2$ into nanostructured $\text{Al}_2\text{O}_3/\text{TiO}_2$ powders. That means the wear resistance of the $\text{Al}_2\text{O}_3/\text{TiO}_2$ coating can be greatly improved by adding different additives even while keeping the hardness almost the same. The dominating mechanism of material removal for the coating sprayed with conventional $\text{Al}_2\text{O}_3/\text{TiO}_2$ powder is grain dislodgment due to grain boundary fracture combined with lateral crack chipping. For the coatings sprayed with nanostructured $\text{Al}_2\text{O}_3/\text{TiO}_2$ powders, the mechanism is mainly grain dislodgment.

(4) There is no simple relationship between the wear resistance and the hardness of the $\text{Al}_2\text{O}_3/\text{TiO}_2$ coatings. It is suggest that the abrasive wear resistance of the $\text{Al}_2\text{O}_3/\text{TiO}_2$ ceramic coatings is strongly dependent on the toughness of the coatings and the process of structural change in the coatings during wear, as well as the density and the hardness of the coatings.

Acknowledgements

The authors would like to thank the financial support provided by the Office of Naval Research under contract #N00014-97-1-0843 and Inframmat Corporation. We are also grateful to Prof. Maurice Gell of the University of Connecticut for helpful discussions and his management in the dense ceramic coating program. Thanks are also due to Prof. Leon Shaw of the University of Connecticut for technical discussions.

References

- [1] Y. Sun, B. Li, D. Yang, T. Wang, Y. Sasaki, K. Ishii, Unlubricated friction and wear behaviour of zirconia ceramics, *Wear* 215 (1998) 232–236.
- [2] J. Knuutila, S. Ahmaniemi, E. Leivo, P. Sorsa, P. Vuoristo, T. Mantylat, Wet abrasion and slurry erosion resistance of sealed oxide coatings, *Proceedings of the 15th International Thermal Spray Conference*, Vol. 1, 25–29 May 1998, Nice, France, pp. 145–150.
- [3] A. Giroud, C. Jouanny, J.L. Heuze, F. Gaillard, P. Guiraldenq, Friction and corrosion behavior of different ceramic coatings (oxides) obtained by thermal spray for qualification tests in sea water, *Proceedings of the 15th International Thermal Spray Conference*, Vol. 1, 25–29 May 1998, Nice, France, pp. 211–216.
- [4] C. Ding, J. Li, L. Zhang, X. Yu, Wear evaluation of plasma sprayed oxide and carbide coatings, *Proceedings of the 15th International Thermal Spray Conference*, Vol. 1, 25–29 May 1998, Nice, France, pp. 275–279.

- [5] M. Cadenas, R. Vijande, H.J. Montes, J.M. Sierra, Wear behaviour of laser clad and plasma sprayed WC–Co coatings, *Wear* 212 (1997) 244–253.
- [6] W.C. Russell, Structure of composite Al_2O_3 – ZrO_2 CVD coatings, in: T.S. Sudarshan, J.F. Braza (Eds.), *Surface Modification Technologies VI*, The Minerals, Metals and Materials Society, 1993, pp. 485–493.
- [7] A.L. Clavel, J. Kyle, CVD coatings and equipment for the metal working industry, in: T.S. Sudarshan, J.F. Braza (Eds.), *Surface Modification Technologies VI*, The Minerals, Metals and Materials Society, 1993, pp. 496–519.
- [8] P.R. Strutt, R.F. Boland, B.H. Kear, Nanostructured feeds for thermal spray systems, methods of manufacture, and coating formed therefrom, US Patent filed, Nov. 1995.
- [9] T.D. Xiao, S. Jiang, D.M. Wang, Y. Wang, R. Zatorski, C.W. Strock, P.R. Strutt, Thermal Spray of Nanostructured Ceramic Coatings for Improved Mechanical properties, 12th Intl. Surface Modification Conference, ASM Intl. 1998, in press.
- [10] Product Bulletins, issued by Metco.
- [11] R.W. Davidge, F.L. Riley, Grain-size dependence of the wear of alumina, *Wear* 186/187 (1995) 45–49.
- [12] H.H.K. Xu, S. Jahanmir, Transitions in the mechanism of material removal in abrasive wear of alumina, *Wear* 192 (1996) 228–232.
- [13] S.-J. Cho, B.J. Hockey, B.R. Lawn, S.J. Bennison, Grain size and *R*-curve effects in the abrasive wear of alumina, *J. Am. Ceram. Soc.* 72 (1989) 1249–1252.
- [14] Y. Wang, T.C. Lei, J.J. Liu, Tribo-metallographic behavior of high carbon steels in dry sliding: I. Wear mechanisms and their transition, *Wear* 231 (1999) 1–17.
- [15] D. Tabor, Wear — a critical synoptic view, in: W.A. Glaeser, et al. (Eds.), *Wear of Materials 1977*, ASME, New York, NY, pp. 1–11.
- [16] S.-J. Cho, H. Moon, B.J. Hockey, S.M. Hsu, The transition from mild to severe wear in alumina during sliding, *Acta Metall. Mater.* 40 (1992) 185–192.
- [17] S. Ramalingam, P.K. Wright, Abrasive wear in machining: experiments with materials of controlled and microstructure, *J. Eng. Mater. Technol.* 103 (1981) 151–156.
- [18] M. Boas, M. Bamberger, Low load abrasive wear behavior of plasma spray and laser-melted plasma coatings, *Wear* 126 (1988) 197–210.
- [19] M.M. Khruschov, Principles of abrasive wear, *Wear* 28 (1974) 49–88.
- [20] H. Liu, M.E. Fine, Modelling of grain-size dependent microfracture-controlled sliding wear in polycrystalline alumina, *J. Am. Ceram. Soc.* 76 (1993) 2392–2396.
- [21] S.M. Wiederhorn, B.J. Hockey, Effect of material parameters on the erosion resistance of brittle materials, *J. Mater. Sci.* 18 (1983) 766–789.
- [22] S. Lathabai, D.D. Pender, Microstructural influence in slurry erosion of ceramics, *Wear* 189 (1995) 122–135.
- [23] A. Erdemir, A review of the lubrication of ceramics with thin solid films, in: S. Jahanmir (Ed.), *Friction and Wear of Ceramics*, Marcel Dekker, New York, 1994, pp. 119–161.
- [24] T.E. Fischer, M.P. Anderson, S. Jahanmir, Influence of fracture toughness on the wear resistance of yttria-doped zirconium oxide, *J. Am. Ceram. Soc.* 72 (1989) 252–257.
- [25] K.-H. Zum Gahr, Modeling and microstructural modification of alumina ceramic for improved tribological properties, *Wear* 200 (1996) 215–224.
- [26] K. Jia, T.E. Fischer, Abrasion resistance of nanostructured and conventional cemented carbides, *Wear* 200 (1996) 206–214.